Title	Accuracy of Le Fort I osteotomy with combined computer-aided design/computer-aided manufacturing technology and mixed reality
Author(s) Alternative	Koyachi, M; Sugahara, K; Odaka, K; Matsunaga, S; Abe, S; Sugimoto, M; Katakura, A
Journal	International journal of oral and maxillofacial surgery, 50(6): 782-790
URL	http://hdl.handle.net/10130/5458
Right	© 2020 The Author(s). Published by Elsevier Ltd on behalf of International Association of Oral and Maxillofacial Surgeons. This is an open access article under the CC BY-NC-ND license (http://creativecommons.org/licenses/by-nc-nd/4.0/).
Description	

Int. J. Oral Maxillofac. Surg. 2021; 50: 782–790
https://doi.org/10.1016/j.ijom.2020.09.026, available online at https://www.sciencedirect.com

International Journal of Oral & Maxillofacial Surgery

Research Paper
Orthognathic Surgery

Accuracy of Le Fort I osteotomy with combined computer-aided design/computer-aided manufacturing technology and mixed reality

M. Koyachi[1], K. Sugahara[1,2], K. Odaka[3], S. Matsunaga[2,4], S. Abe[2,4], M. Sugimoto[1,5], A. Katakura[1,2]

[1]Department of Oral Pathobiological Science and Surgery, Tokyo Dental College, Tokyo, Japan; [2]Oral Health Science Centre, Tokyo Dental College, Tokyo, Japan; [3]Department of Oral and Maxillofacial Radiology, Tokyo Dental College, Tokyo, Japan; [4]Department of Anatomy, Tokyo Dental College, Tokyo, Japan; [5]Okinaga Research Institute Innovation Laboratory, Teikyo University, Tokyo, Japan

M. Koyachi, K. Sugahara, K. Odaka, S. Matsunaga, S. Abe, M. Sugimoto, A. Katakura: Accuracy of Le Fort I osteotomy with combined computer-aided design/computer-aided manufacturing technology and mixed reality. Int. J. Oral Maxillofac. Surg. 2021; 50: 782–790.

Abstract. The aim of this study was to verify the reproducibility and accuracy of preoperative planning in maxilla repositioning surgery performed with the use of computer-aided design/manufacturing technologies and mixed reality surgical navigation, using new registration markers and the HoloLens headset. Eighteen patients with a mean age of 26.0 years were included. Postoperative evaluations were conducted by comparing the preoperative virtual operation three-dimensional image (Tv) with the 1-month postoperative computed tomography image (T_1). The three-dimensional surface analysis errors ranged from 79.9% to 97.1%, with an average error of 90.3%. In the point-based analysis, the errors at each point on the *XYZ* axes were calculated for Tv and T_1 in all cases. The median signed value deviation of all calculated points on the *XYZ* axes was −0.03 mm (range −2.93 mm to 3.93 mm). The median absolute value deviation of all calculated points on the *XYZ* axes was 0.38 mm (range 0 mm to 3.93 mm). There were no statistically significant differences between any of the points on any of the axes. These values indicate that the method used was able to reproduce the maxilla position with high accuracy.

Key words: augmented reality; computer-aided design; computer-assisted surgery; orthognathic surgery; Le Fort osteotomy.

Accepted for publication
Available online 3 November 2020

The Le Fort I osteotomy is a highly effective treatment for skeletal jaw deformities. The double splint modification of the Le Fort I osteotomy, introduced by Lindorf and Steinhäuser[1], is highly effective for recreating a mould-based model during surgery and is used widely on a global scale. However, Mazzoni et al.[2] and Sharifi et al.[3] have reported that the accuracy of maxilla repositioning during the Le Fort I osteotomy procedure using the double splint method is dependent on the technical expertise of the

0901-5027/060782 + 09

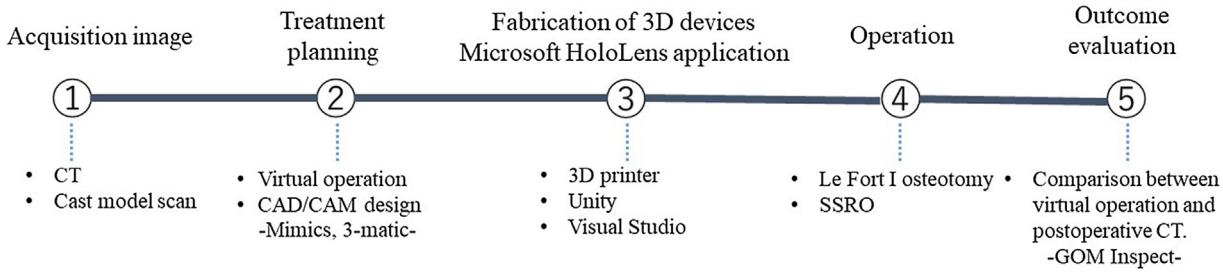

Fig. 1. Workflow of this study.

surgeon, and that errors from the preoperative model planning stage can occur during facebow transfer and splint fabrication. Tominaga et al.[4] reported that the accuracy of maxillofacial surgery can be improved by fabricating a preoperative bone fragment positioning guide. However, even with these additional techniques, the expertise and experience of the surgeon play a large role in the patient prognosis. For this reason, there is great demand for the development of a system that accurately recreates the quantitatively evaluated treatment plan during surgery.

In recent years, surgical disciplines have been in the midst of a paradigm shift due to the rapid development of surgical navigation techniques that utilize digital equipment. Wong et al.[5] conducted surgical navigation using three-dimensional (3D) moulds created by a 3D printer, and this method has shown a certain degree of success in orthopaedic disciplines. Regarding splint-guided osteotomies, Park et al. reported good results for orthognathic surgery using computer-aided design/computer-aided manufacturing (CAD/CAM) guides, but they could be more accurate[6].

Reports have indicated that head-mounted displays (HMDs) with installed mixed reality (MR) techniques can confirm the location of vascular pedunculated flaps, thus minimizing the risk of haemorrhage from small veins[7]. Despite these advancements, the success or failure of surgery in the maxillofacial area may be determined by small-scale differences; therefore, a specialized and extremely accurate system is necessary.

Therefore, the aim of this study was to investigate the accuracy of the Le Fort I osteotomy procedure performed using CAD/CAM surgical guides and new registration markers for MR surgical navigation and to verify the reproducibility of the preoperative plan.

Materials and methods

The procedure performed in this study was conducted using six steps, which are outlined below and shown in Fig. 1: (1) acquisition of the skull data from computed tomography (CT) and the dentition from laser scanning; (2) treatment planning via the creation of a skull–dental composite 3D model and a digital dental model, in addition to virtual surgery; (3) fabrication of 3D devices and creation of the Microsoft HoloLens application; (4) performance of the actual operation based on the virtual operation; and (5) evaluation of the accuracy of the operation by comparison of the virtual operation with the postoperative CT.

Study population

Details of the study subjects are given in Table 1. Eighteen patients were included in this study; they ranged in age from 17 to 45 years, with a mean age of 26.0 years. The surgeries were conducted in the Oral Surgery Department of Suidobashi Hospital, Tokyo Dental College from October 2018 to October 2019. Patients with a cleft palate or craniofacial abnormality were excluded from this study. The study was approved by the Ethics Committee of Tokyo Dental College (No. 794 844).

Table 1. Clinical information for the study patients and the results of the three-dimensional surface analysis.

Patient	Age (years)	Diagnosis	Surgical treatment for maxilla	Error <2 mm (%)[a]
1[b]	24	FA, CB	Advancement, right up, left down	97.1
2	30	RU, PL, ACB	Advancement, anticlockwise rotation	89.5
3[b]	38	FA, CB	Right down, left up	92.9
4	24	RU, PL	Advancement	79.9
5[b]	21	FA, CB	Left shift, left down	95.0
6	25	RU, PL, ACB	Advancement	93.3
7[b,c]	26	FA, AOB	Right up, left up	92.0
8[b,c]	36	FA, RL, DB	Right up, left up	95.6
9[b,c]	28	FA, PL, AOB	Right shift, right up	90.3
10	28	PU, RL, DB	Setback, anticlockwise rotation	88.9
11[b,c]	45	FA, AOB	Right up	96.1
12[b,c]	24	FA, PL, ACB	Right down, left up, impaction	84.0
13[c]	17	RU, PL, ACB	Advancement, left shift, impaction	81.5
14[c]	17	PU, RL, AOB	Anticlockwise rotation	82.5
15[b]	19	FA, PL, ACB	Setback, right shift, right up	91.3
16	20	RU, PL, ACB	Advancement	93.6
17[b]	26	FA, PL, ACB	Right shift, left down	91.1
18	20	RU, PL	Advancement, right down, left down	90.0

ACB, anterior crossbite; AOB, anterior open bite; CB, crossbite; DB, deep bite; FA, facial asymmetry; PL, prognathia of lower jaw; PU, prognathia of upper jaw; RL, retrognathia of lower jaw; RU, retrognathia of upper jaw.

[a] The average percentage of bone errors of <2 mm between the Tv and T_1 images was 90.3%.

[b] Cases with tilt improvement.

[c] Cases with vertical repositioning of the posterior nasal spine (PNS).

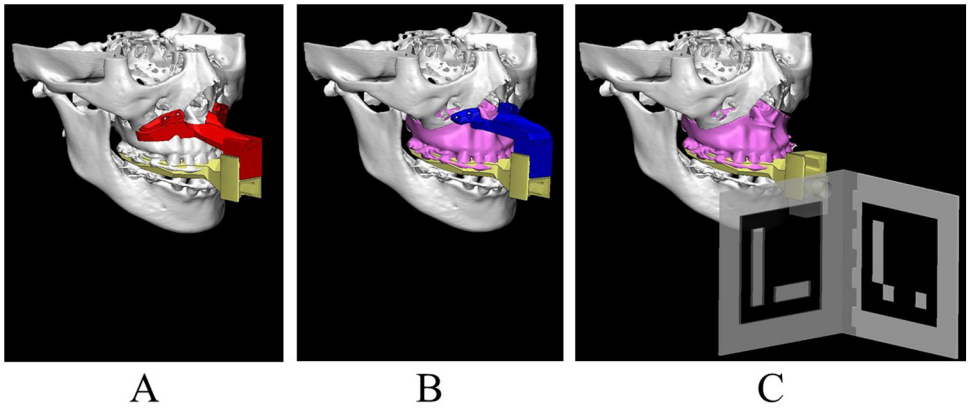

Fig. 2. Computer-aided design of the 3D devices: (A) splint (yellow) and osteotomy device (red); (B) repositioning device (blue); (C) registration marker. The osteotomy device and repositioning device were made so that they could be attached to the splint and switched in or out at the upper junction site. The registration marker could be attached to the lower junction site.

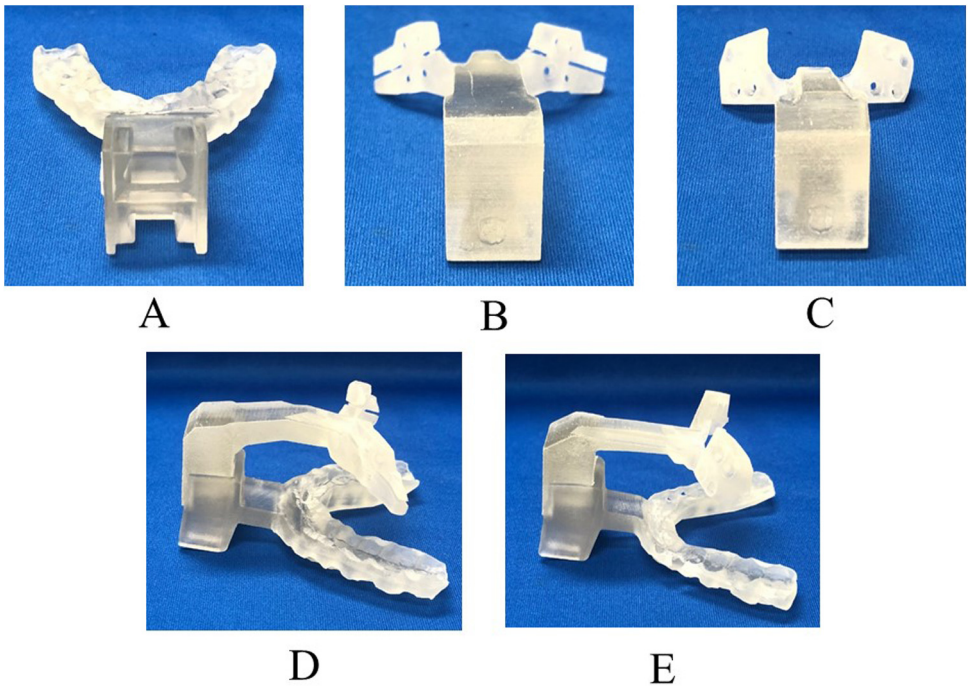

Fig. 3. 3D devices made by computer-aided manufacturing: (A) surgical splint; (B) osteotomy device; (C) repositioning device; (D) surgical splint connected to the osteotomy device; (E) surgical splint connected to the repositioning device. The osteotomy device and repositioning guide were customized in each case.

Image acquisition

CT scans (SOMATOM Definition AS; Siemens, Forchheim, Germany) were obtained a month prior to surgery, and the CT images were formatted as DICOM data. Since accurate reconstruction of the dentition is difficult due to orthodontic brackets and prosthetic artefacts, a digital impression of a plaster cast was scanned (D2000; 3Shape, Szczecin, Poland) and converted into STL data format. The CT DICOM and digital impression data were transferred to Mimics (Materialise, Leuven, Belgium) and 3-matic (Materialise, Leuven, Belgium) and set up to allow the virtual operation.

Preoperative procedure—3D devices

The CT data and dentition mould were aligned using Mimics and 3-matic. The superimposition of the CT data and the dentition model data was performed using any three points on the tooth incisal and occlusal surfaces that could be clearly confirmed. The extent of the maxilla repositioning was determined from these data following discussions with the orthodontists, and the surgeon determined the osteotomy incision lines and designed the osteotomy device, repositioning device, splint, and registration markers. These data were converted into STL format, and each 3D device was fabricated using a 3D printer (Objet 260 Connex; Stratasys Ltd, Eden Prairie, MN, USA). The osteotomy device and repositioning device were made so that they could be attached to the splint and switched in or out at this junction site. No screws or adhesives were used at the junction site; instead a 'Koshikakearitsugi' (i.e., a stepped dovetail splice) configuration, which is used in shrine carpentry techniques, was applied. It was ensured that the attachment was secure by maintaining an open window to the upper section adjacent to the anterior nasal spine (ANS) (Figs 2 and 3).

Preoperative procedure—Microsoft HoloLens

The virtual reality (VR) application was created using Unity 2017.4.17 (Unity

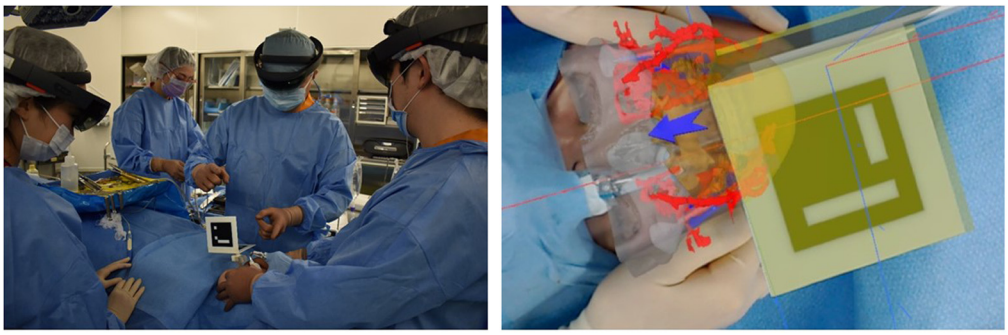

Fig. 4. Intraoperative view: (A) operators wearing HoloLens headsets can share the hologram and manipulate it using gestures and voice commands; (B) the operating field and the application can be aligned automatically by fabricating the markers, and the HoloLens device recognizes the markers.

Technologies, San Francisco, CA, USA), Visual Studio Community 2017/version 15.9.4 (Microsoft Corp., Redmond, WA, USA), and OpenCV 3.1 (Open Source Computer Vision Library) + ArUco software (AVA Group, University of Córdoba, Córdoba, Spain). The hologram reconstructs the skull, the pre- and post-repositioned maxilla/mandible, the markers, and the arteries/veins from the contrast CT scans. Each VR could modify movement, rotation, and transparency with gestural movements, which was useful for confirmation when the patient and the application were aligned. Additionally, the displays of each VR could be toggled on or off. The maxillary bone could be chosen from two VR types (pre- and post-repositioning). Furthermore, the operating field and the application could be automatically aligned by fabricating the markers used for alignment with the 3D printer, and the HoloLens recognized the markers attached to the splint in our application. The surgeon could confirm the marker, and the system was designed with two surfaces (surface size = 10 × 10 cm) that did not interfere with the operating field (Fig. 4).

Surgical procedure

All surgeries were performed by a single specialist oral and maxillofacial surgeon. The directions of the movements of the Le Fort I segment are reported in Table 1. In all Le Fort I osteotomies, an incision was applied from the right maxillary second premolar to the left maxillary second premolar. The splint was fitted onto the maxilla and the osteotomy device was mounted at the junction site. In addition, a screw was inserted and temporarily fixed into the screw hole. The osteotomy device was removed and the maxilla was down-fractured after an osteotomy had been performed on both the lateral and medial sides of the maxilla. The osteotomy device was then switched to the repositioning device, and the maxilla was repositioned so that the screw could be inserted into the screw hole, after which the maxilla was fixed using two metal six-hole plates from the bilateral zygomatic buttress. The registration marker was connected to the splint junction site, and once the repositioning of the maxilla was confirmed in 3D to be that specified by the virtual operation with the HoloLens, the repositioning device was removed and the maxilla was fixed to the buttress of the piriform margin using two resorbable five-hole plates.

Evaluation

Postoperative evaluations were conducted by comparing the preoperative virtual operation 3D image (Tv) with the 1-month postoperative CT image (T_1) using Materialise Mimics and 3-matic. Overlaying and evaluation of the Tv and T_1 images were conducted using GOM Inspect (GOM, Braunschweig, Germany). The skull, which was unaffected during surgery, was used as a reference for image overlaying, and three arbitrary points were automatically selected following setup[8]. The reference plane was established using the methods of Badiali et al.[9] and Park et al.[10]: the 3D-CT centre was set as the middle point between the porion (Po) on both sides, the *X*-axis was set as the middle

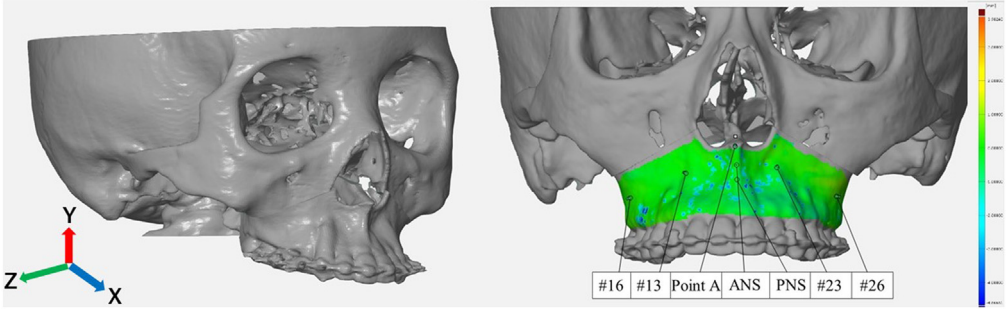

Fig. 5. Reference plane and postoperative evaluations: (A) the reference plane was established, where the 3D-CT centre was set as the middle point between the porions on both sides, the *X*-axis was set as the middle point that passes between the orbitales on both sides, the *Y*-axis was set as the vertical cranial direction from the Frankfort horizontal plane, and the *Z*-axis was set as the right-hand direction from the centre; (B) a 3D surface analysis and a point-based analysis were used as the methods of evaluation. The points evaluated were as follows: A-point, anterior nasal spine (ANS), posterior nasal spine (PNS), centre of the maxillary central incisor root apex, the canine root apex on both sides (#13 and #23), and the first molar root apex on both sides (#16 and #26).

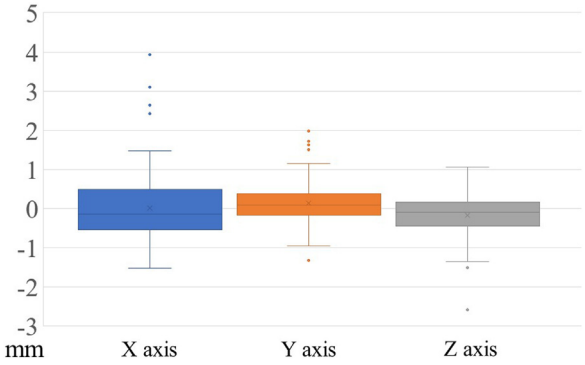

Fig. 6. Signed value deviation between Tv and T_1. The accuracy at each point was calculated with regard to the *XYZ* axes. Positive values represent under-correction and negative values represent over-correction of the planned maxillary position.

point that passes between the orbitale (Or) on both sides, the *Y*-axis was set as the vertical cranial direction from the Frankfort horizontal (FH) plane, and the *Z*-axis was set as the right-hand direction from the centre, with the *X*/*Z* plane set up to be aligned with the FH plane. Since only the bone surfaces were being compared, the metallic plate sections in the postoperative CT were removed using the methods outlined by Badiali et al.[9]. A 3D surface analysis and a point-based analysis were used as the methods of evaluation (Fig. 5). The absolute values and signed values were used[11]. The absolute values express the absolute accuracy of the method, and the signed values express an under (+ value) or over (− value) correction.

3D surface analysis

Errors between the Tv and T_1 bone surfaces were measured. Based on previous reports, the threshold value was set at <2 mm, and the percentage of errors under this value was calculated[12–14].

Point-based analysis

The points evaluated were as follows: A-point, ANS, posterior nasal spine (PNS), centre of the maxillary central incisor root apex, the canine root apex on both sides (#13 and #23), and the first molar root apex on both sides (#16 and #26). Tv and T_1 were compared, and the distance errors on each axis ($Xv - X_1$, $Yv - Y_1$, $Zv - Z_1$) were measured. The measurements were performed twice by the same operator, and the average value was used as the evaluation value. The intra-class correlation coefficient was determined for the two sets of Tv measurements and for the two sets of T_1 measurements; the correlation coefficient in each case was greater than 0.99. Regarding the influence of postoperative correction, the root apex was used as the evaluation criterion[15].

Statistical analysis

All statistical analyses were performed using IBM SPSS Statistics version 23.0 (IBM Corp., Armonk, NY, USA). The Mann–Whitney *U*-test and Kruskal–Wallis test were used to compare the Tv and T_1 images. Statistical significance was set at $P < 0.05$.

Results

3D surface analysis

The results of the 3D surface analysis are reported in Table 1. The percentage of bone measurement error within 2 mm between the Tv and T_1 images ranged from 79.9% to 97.1%, with an average error of 90.3%. The accuracy was >90.0% in 12 cases.

Point-based analysis

Signed values

The errors at each point on the *XYZ* axes were calculated for Tv and T_1 in all cases. The median signed value deviation of all calculated points on the *XYZ* axes was −0.03 mm (range −2.93 mm to 3.93 mm) (Fig. 6).

The signed value was a median of −0.14 mm (range −1.52 mm to 3.93 mm) on the *X*-axis, 0.10 mm (range −2.93 mm to 3.24 mm) on the *Y*-axis, and −0.09 mm (range −2.59 mm to 1.42 mm) on the *Z*-axis. The median error for each axis when comparing Tv and T_1 was within 2 mm. The signed value deviation for ANS varied widely on the *X*-axis, from −0.42 to 3.93 mm. The signed value deviation for PNS had the largest range on the *Y*-axis, from −2.93 to 3.24 mm (Fig. 7). There were no statistically significant differences between Tv and T_1 for any of the points on any of the axes (Table 2). Comparisons between the axes showed no statistically significant difference between the *X* and *Z* axes ($P > 0.05$), but statistically significant differences were observed between the *X* and *Y* axes($P < 0.05$) and between the *Y* and *Z* axes ($P < 0.05$).

Absolute values

The median absolute value deviation of all calculated points on the *XYZ* axes was 0.38 mm (range 0 mm to 3.93 mm) (Fig. 8).

The absolute value was a median of 0.56 mm (range 0–3.93 mm) on the *X*-axis, 0.29 mm (range 0.01–3.24 mm) on the *Y*-axis, and 0.33 mm (range 0–2.59 mm) on the *Z*-axis (Fig. 8). The absolute value also showed that the median error for each axis (comparison between Tv and T_1) was within 2 mm. Similar to the signed values, the accuracy tended to be lower for ANS on the *X*-axis and PNS on the *Y*-axis (Fig. 9). Comparisons between the axes showed no statistically significant differences between the *Y* and *Z* axes ($P > 0.05$), but statistically significant differences were observed between the *X* and *Y* axes ($P < 0.05$) and between the *X* and *Z* axes ($P < 0.05$).

Registration to participate in this study did not result in any delay in surgery, and the duration of the surgical procedure was relatively unaffected because the surgeon began the surgery while wearing the HoloLens headset. Additionally, the surgeon could smoothly operate the surgical guide in all cases. No abnormal haemorrhaging or fractures were observed during the procedure for any of the patients.

Discussion

With the development of computer-aided surgical simulation in the oral and maxillofacial region, there have been numerous discussions on the effectiveness of conducting preoperative virtual operations from clinical imaging data (e.g., CT)[16]. For the Le Fort I osteotomy procedure in particular, the application of 3D printing and use of patient-specific implants (PSIs) produced by 3D metal printing have been utilized to determine the maxilla position[15,17]. PSIs produced by 3D metal printing have not yet been clinically approved in Japan; thus, 3D printers that use biocompatible materials have become mainstream for surgical guides, similar to what is outlined in the current report.

Additionally, image-guided surgery (IGS) has been reported, where 3D recon-

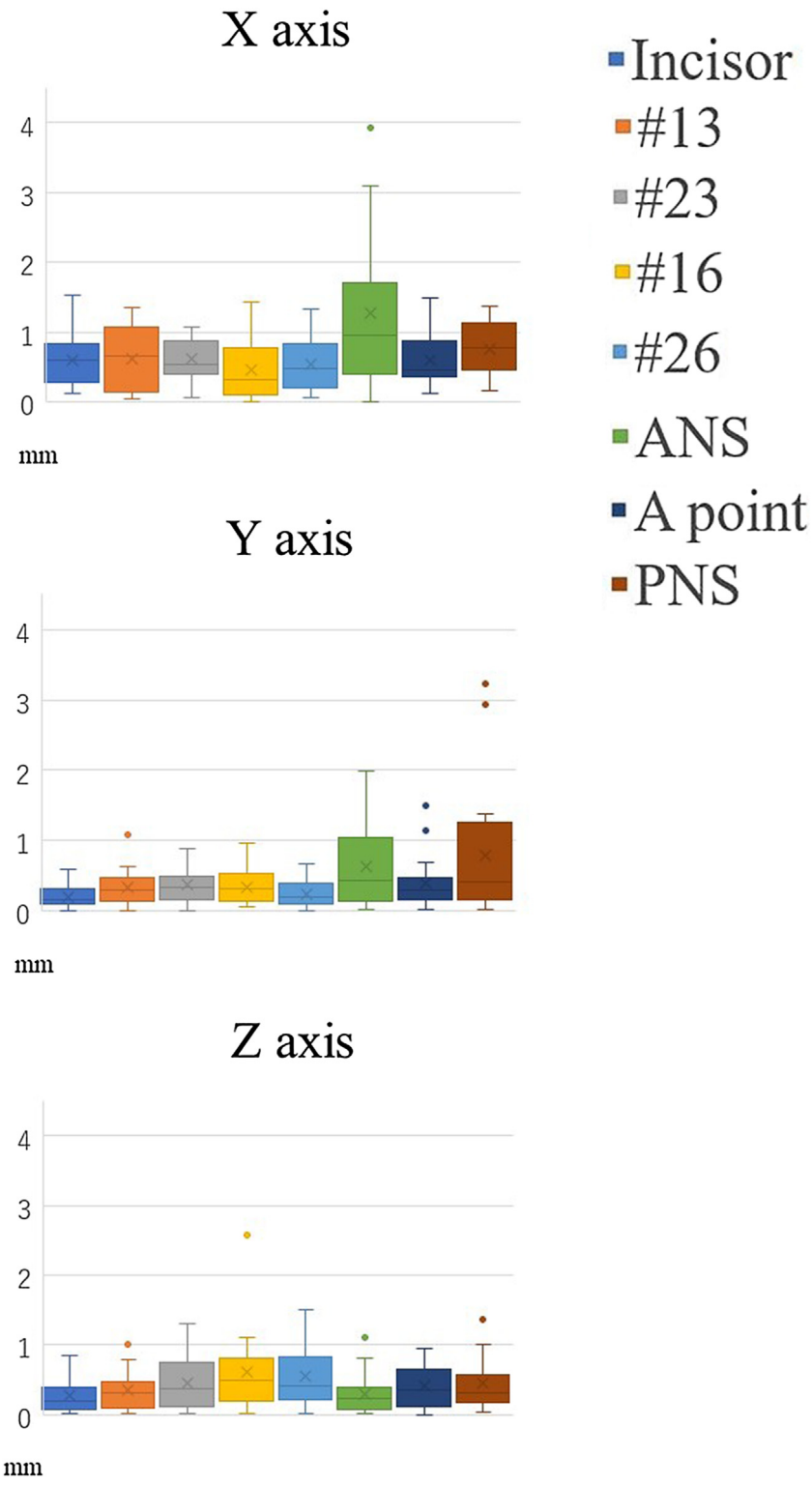

Fig. 7. Signed value deviation between Tv and T_1 at each point on the *XYZ* axes. An error of +3.93 mm was observed for ANS on the *X*-axis, and an error of +1.98 mm for ANS and 3.24 mm for PNS was observed on the *Y*-axis.

structions of the clinical imaging data are made; anatomical structures such as blood vessels, nerves, and bones are confirmed, and the spatial relationships between the surgical tools and patients can be confirmed in real-time with surgical navigation[9]. A recent study discussed a case in which waferless navigation based on augmented reality (AR) was applied as an IGS technique to a Le Fort I osteotomy procedure[18]. However, IGS guides the maxillary repositioning and confirmation through a monitor and is thus two-dimensional in nature.

The Microsoft HoloLens has recently been applied to surgical navigation, however almost no applications of this technology in the field of oral surgery have

Table 2. Signed value deviation between Tv and T_1 at each point: range, median, and results of the statistical analysis.

	$Xv - X_1$			$Yv - Y_1$			$Zv - Z_1$		
	Range (mm)	Median (mm)	*P*-value	Range (mm)	Median (mm)	*P*-value	Range (mm)	Median (mm)	*P*-value
Incisor	−1.52 to 0.80	−0.32	0.79	−0.28 to 0.59	0.09	0.91	−0.84 to 0.23	−0.07	0.63
#13	−1.35 to 1.12	−0.16	0.61	−0.59 to 1.08	−0.01	1.00	−1.01 to 0.74	−0.04	0.94
#23	−1.07 to 1.04	−0.40	0.79	−0.45 to 0.88	0.25	0.70	−1.30 to 0.84	−0.32	0.56
#16	−1.43 to 1.35	−0.09	0.91	−0.96 to 0.66	0.02	1.00	−2.59 to 1.06	−0.19	0.74
#26	−1.33 to 0.99	−0.35	0.77	−0.68 to 0.56	0.05	0.82	−1.51 to 0.94	−0.06	0.89
ANS	−0.42 to 3.93	0.95	0.65	−1.32 to 1.98	0.41	0.74	−1.11 to 0.64	0.01	0.86
A-point	−1.50 to 1.26	0.03	0.99	−0.61 to 1.50	0.01	0.89	−0.94 to 0.63	−0.11	0.65
PNS	−1.38 to 1.20	−0.53	0.72	−2.93 to 3.24	0.08	0.74	−1.00 to 1.42	0.04	0.94

ANS, anterior nasal spine; PNS, posterior nasal spine.
For all points, the median error between the preoperative virtual operation and the 1-month postoperative CT data was less than 2 mm, with no significant differences. Hence, it is considered that the surgery was performed with an accuracy close to the preoperative virtual operation.

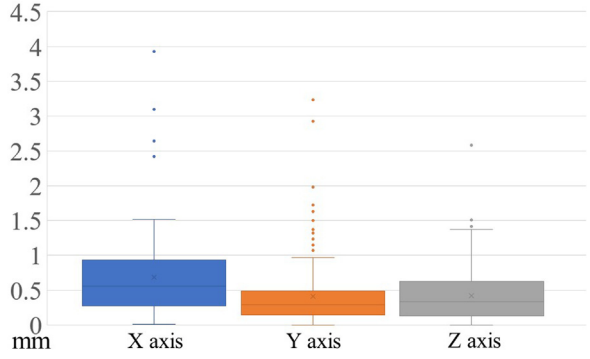

Fig. 8. Absolute value deviation between Tv and T_1. The accuracy at each point with regard to the *XYZ* axes was calculated. The median absolute value for each axis was as follows: 0.56 mm (range 0–3.93 mm) on the *X*-axis, 0.29 mm (range 0.01–3.24 mm) on the *Y*-axis, and 0.33 mm (range 0–2.59 mm) on the *Z*-axis.

been noted. Surgeons using the Microsoft HoloLens can maintain the 3D hologram reconstructed from clinical imaging data on the operating field without breaking eye contact and can conduct surgery while continuing to look at the patient[19]. Standard AR and navigation systems have limitations regarding portability, calibration, and tracking, and their costs can be prohibitively high. In contrast, MR-HMDs, such as the Microsoft HoloLens, are easy to carry, project an accurate hologram in space, and operations can be conducted through gestural movements. Additionally, sanitary operations can be conducted due to the gestural nature of the procedure. As seen above, the limitations imposed during surgery are gradually disappearing[20].

Up to now, only a few studies have included a control group, and many have compared the preoperative virtual operation 3D image and the postoperative CT image[2,11,19]. One of the clinical goals is to achieve an error of less than 2 mm between the virtual operation 3D image and the postoperative CT image[21]. In this study, the analysis showed a 3D surface accuracy ranging from 79.9% to 97.1%, with an average of 90.3%. Previous reports of Le Fort I osteotomies performed using image-based aids or a 3D-printed metal PSI have reported bone surface alignment errors <2 mm of between 62% and 100%, with an average of 83.8% to 92.7%[2,9]. These values indicate that the method used in the present study was able to reproduce the maxilla position with high accuracy.

The point-based analysis of the current application showed that the median error for each axis when comparing Tv and T_1 was <2 mm, and no statistically significant differences were observed between Tv and T_1 for any of the points on any of the axes. The error in positioning the maxilla using a wafer made from a conventional cast model was approximately 5 mm[22]. Thus, the maxilla was considered to have been repositioned as specified by the preoperative virtual operation.

Regarding the direction of movement of the maxilla, high accuracy was observed in the tilt improvement cases (Table 1). Similar to previous reports, a lower accuracy was observed in specific tilt improvement cases, such as in bone repositioning in the impaction direction (Table 1), and in vertical repositioning of the PNS (Table 1)[11]. It is thought that in these cases, it was difficult to trim the obstructed area, such as the area in the vicinity of the descending palatine artery, when repositioning the maxilla as specified by the virtual operation, even with CAD/CAM usage; impaction cannot occur in the expected location during maxilla repositioning. As a result, it is thought that when comparing each axis, significant *Y*-axis differences were observed in the signed value because under-correction was more likely to occur in the *Y*-axis than in the other axes. In some cases, negative values in the *X*-axis direction for ANS and A-point were thought to be possibly due to infiltration in the ANS section from mucosal abrasion during surgery, or the presence of compressed bone resorption due to drilling in the ANS following alar base cinch sutures to control alar expansion, and it being ligated with an absorbable suture. Therefore, the accuracy of the absolute value tends to be lower for ANS on the *X*-axis, and it is possible that a significant difference occurs in the absolute value when comparing the *Y* and *Z* axes; thus, we considered that the ANS tended to be influenced as a measurement item in this study.

The HoloLens was used to confirm reproducibility after maxilla repositioning in the study method; however, the above results were likely due to the fact that although patient/hologram alignment errors can be detected fairly easily, including tilt improvement cases where confirmation can be done from the front side, PNS repositioning confirmation is conducted from the lateral side. Recent studies have calculated that errors in physical object/hologram alignment due to the HoloLens are on average 2.5 mm[23] or 2.77 mm[24], and it is currently believed that the determination of maxilla position using only HMDs is difficult. So guided surgery using only MR is ideal, but in this study, MR was used to improve the accuracy of CAD/CAM surgical guides. For this reason, we sought to increase accuracy by confirming in 3D and by the symmetry of the Le Fort I segment during the operation that the maxilla was repositioned as specified in the preoperative

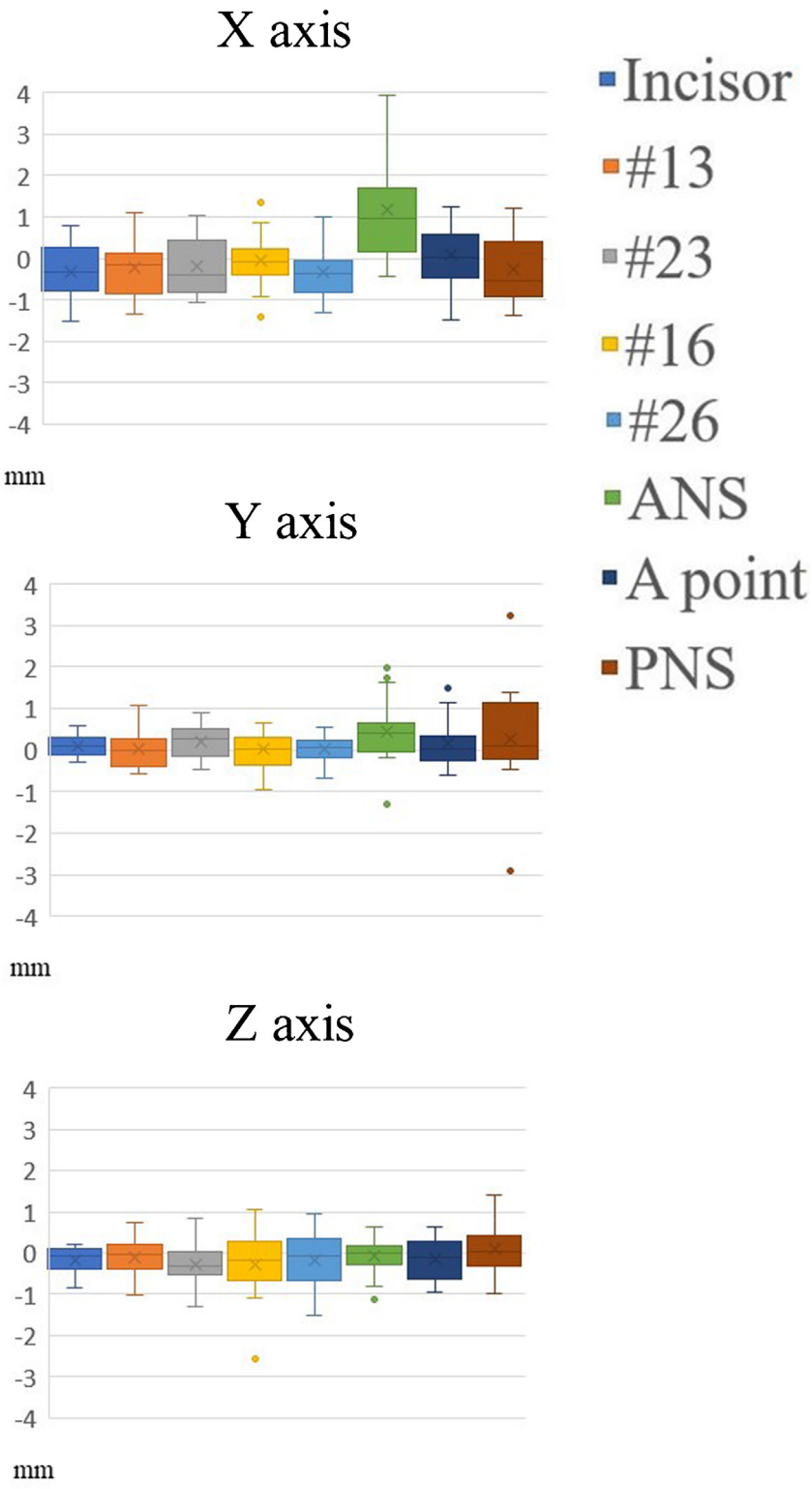

Fig. 9. Absolute value deviation between Tv and T_1 at each point on the *XYZ* axes. Similar to the signed values, the accuracy tended to be lower for ANS on the *X*-axis and PNS on the *Y*-axis.

virtual operation by combining the HoloLens with CAD/CAM-fabricated splints. Therefore, the accuracy is further improved by using MR. This method appears to be novel as it can be used to check intraoperatively using MR that the planned maxillary positioning (as determined from the virtual operation) can be performed using the CAD/CAM manufactured devices.

In this study, the preoperative virtual operation was recreated with high accuracy by combining MR and CAD/CAM techniques. Compared to previous studies, the 3D surface and point-based analyses indicate that this method was able to reproduce the maxillary position with a high level of accuracy on all axes. Additionally,

surgical navigation using only MR is currently difficult due to the high level of accuracy needed for surgical jaw correction; however, MR can be used as a checking device during surgery by combining it with CAD/CAM-fabricated splints, as performed in the current study.

Funding

Not applicable.

Competing interests

The authors declare no conflict of interest.

Ethical approval

The study was approved by the Ethics Committee of Tokyo Dental College, Tokyo, Japan (No. 794 844).

Patient consent

Written patient consent was obtained.

Acknowledgements. We wish to thank Holoeyes Inc. for technical support during the creation of the MR application and Meishin Electric Co., Inc. for the appropriate design of the devices.

References

1. Lindorf HH, Steinhäuser EW. Correction of jaw deformities involving simultaneous osteotomy of the mandible and maxilla. *J Maxillofac Surg* 1978;**6**:239–44.
2. Mazzoni S, Bianchi A, Schiariti G, Badiali G, Marchetti C. Computer-aided design and computer-aided manufacturing cutting guides and customized titanium plates are useful in upper maxilla waferless repositioning. *J Oral Maxillofac Surg* 2015;**73**:701–7. http://dx.doi.org/10.1016/j.joms.2014.10.028.
3. Sharifi A, Jones R, Ayoub A, Moos K, Walker F, Khambay B, McHugh S. How accurate is model planning for orthognathic surgery? *Int J Oral Maxillofac Surg* 2008;**37**:1089–93. http://dx.doi.org/10.1016/j.ijom.2008.06.011.
4. Tominaga K, Yoshioka I, Khanal A, Furuta N, Habu M, Fukuda J. A simple method for bone positioning of mandibular segments. *Int J Oral Maxillofac Surg* 2006;**35**:856–60. http://dx.doi.org/10.1016/j.ijom.2006.03.004.
5. Wong KC, Kumta SM, Sze KY, Wong CM. Use of a patient-specific CAD/CAM surgical jig in extremity bone tumor resection and custom prosthetic reconstruction. *Comput Aid Surg* 2012;**17**:284–93. http://dx.doi.org/10.3109/10929088.2012.725771.
6. Park JH, Yong BL, Sang YK, Hyung JK, Young SJ, Hwi DJ. Accuracy of modified CAD/CAM generated wafer for orthognathic surgery. *PLoS One* 2019;**14**: e0216945. http://dx.doi.org/10.1371/journal.pone.0216945.
7. Pratt P, Ives M, Lawton G, Simmons J, Radev N, Spyropoulou L, Amiras D. Through the HoloLens™ looking glass: augmented reality for extremity reconstruction surgery using 3D vascular models with perforating vessels. *Eur Radiol Exp* 2018;**2**:2. http://dx.doi.org/10.1186/s41747-017-0033-2.
8. Xia JJ, Gateno J, Teichgraeber JF, Christensen AM, Lasky RE, Lemoine JJ, Liebschner MA. Accuracy of the computer-aided surgical simulation (CASS) system in the treatment of patients with complex craniomaxillofacial deformity: a pilot study. *J Oral Maxillofac Surg* 2007;**65**:248–54. http://dx.doi.org/10.1016/j.joms.2006.10.005.
9. Badiali G, Roncari A, Bianchi A, Taddei F, Marchetti C, Schileo E. Navigation in orthognathic surgery: 3D accuracy. *Facial Plast Surg* 2015;**31**:463–73. http://dx.doi.org/10.1055/s-0035-1564716.
10. Park SH, Yu HS, Kim KD, Lee KJ, Baik HS. A proposal for a new analysis of craniofacial morphology by 3-dimensional computed tomography. *Am J Orthod Dentofacial Orthop* 2006;**129**:600.e23–e. http://dx.doi.org/10.1016/j.ajodo.2005.11.032.
11. Heufelder M, Wilde F, Pietzka S, Mascha F, Winter K, Schramm A, Rana M. Clinical accuracy of waferless maxillary positioning using customized surgical guides and patient specific osteosynthesis in bimaxillary orthognathic surgery. *J Craniomaxillofac Surg* 2017;**45**:1578–85. http://dx.doi.org/10.1016/j.jcms.2017.06.027.
12. Ong TK, Banks RJ, Hildreth AJ. Surgical accuracy in Le Fort I maxillary osteotomies. *Br J Oral Maxillofac Surg* 2001;**39**:96–102. http://dx.doi.org/10.1054/bjom.2000.0577.
13. Mazzoni S, Badiali G, Lancellotti L, Babbi L, Bianchi A, Marchetti C. Simulation-guided navigation: a new approach to improve intraoperative three-dimensional reproducibility during orthognathic surgery. *J Craniofac Surg* 2010;**21**:1698–705. http://dx.doi.org/10.1097/SCS.0b013e3181f3c6a8.
14. Marchetti C, Bianchi A, Bassi M, Gori R, Lamberti C, Sarti A. Mathematical modeling and numerical simulation in maxillo-facial virtual surgery (VISU). *J Craniofac Surg* 2006;**17**:661–7. http://dx.doi.org/10.1097/00001665-200607000-00009.
15. Kim JW, Kim JC, Jeong CG, Cheon KJ, Cho SW, Park IY, Yang BE. The accuracy and stability of the maxillary position after orthognathic surgery using a novel computer-aided surgical simulation system. *BMC Oral Health* 2019;**19**:18. http://dx.doi.org/10.1186/s12903-019-0711-y.
16. Keeve E, Girod S, Girod B, Deformable modeling of facial tissue for craniofacial surgery simulation.Höhne KH, Kikinis R, editors. *Visualization in biomedical computing*, vol. 1131. Springer; 1996. p. 541–6. http://dx.doi.org/10.1007/BFb0046996.
17. Zhang N, Liu S, Hu Z, Hu J, Zhu S, Li Y. Accuracy of virtual surgical planning in two-jaw orthognathic surgery: comparison of planned and actual results. *Oral Surg Oral Med Oral Pathol Oral Radiol* 2016;**122**:143–51. http://dx.doi.org/10.1016/j.oooo.2016.03.004.
18. Zinser MJ, Mischkowski RA, Dreiseidler T, Thamm OC, Rothamel D, Zöller JE. Computer-assisted orthognathic surgery: waferless maxillary positioning, versatility, and accuracy of an image-guided visualisation display. *Br J Oral Maxillofac Surg* 2013;**51**:827–33. http://dx.doi.org/10.1016/j.bjoms.2013.06.014.
19. Witowski J, Darocha S, Kownacki , Pietrasik A, Pietura R, Banaszkiewicz M, Kamiński J, Biederman A, Torbicki A, Kurzyna M. Augmented reality and three-dimensional printing in percutaneous interventions on pulmonary arteries. *Quant Imaging Med Surg* 2019;**9**:23–9. http://dx.doi.org/10.21037/qims.2018.09.08.
20. Kress BC, Cummings WJ. 11-1: Invited Paper: Towards the ultimate mixed reality experience: HoloLens display architecture choices. *SID Symposium Digest of Technical Papers* 2017:127–31. http://dx.doi.org/10.1002/sdtp.11586. 48.
21. Stokbro K, Aagaard E, Torkov P, Bell RB, Thygesen T. Virtual planning in orthognathic surgery. *Int J Oral Maxillofac Surg* 2014;**43**:957–65. http://dx.doi.org/10.1016/j.ijom.2014.03.011.
22. Ellis E. Accuracy of model surgery: evaluation of an old technique and introduction of a new one. *J Oral Maxillofac Surg* 1990;**48**:1161–7. http://dx.doi.org/10.1016/0278-2391(90)90532-7.
23. Gibby JT, Swenson SA, Cvetko S, Rao R, Javan R. Head-mounted display augmented reality to guide pedicle screw placement utilizing computed tomography. *Int J Comput Assist Radiol Surg* 2018;**14**:525–35. http://dx.doi.org/10.1007/s11548-018-1814-7.
24. Liebmann F, Roner S, von Atzigen M, Scaramuzza D, Sutter R, Snedeker J, Farshad M, Fürnstahl P. Pedicle screw navigation using surface digitization on the Microsoft HoloLens. *Int J Comput Assist Radiol Surg* 2019;**14**:1157–65. http://dx.doi.org/10.1007/s11548-019-01973-7.

Address:
Masahide Koyachi
Department of Oral Pathobiological Science and Surgery
Tokyo Dental College
2-9-18 Misaki-cho
Chiyoda-ku
101-0061 Tokyo
Japan
Tel.: +81 3 6380 9246;
Fax: +81 3 3262 3213
E-mail: koyachim@tdc.ac.jp